Organic & Biomolecular Chemistry

Cite this: *Org. Biomol. Chem.*, 2012, **10**, 5598

www.rsc.org/obc

PAPER

A theoretical study of carbon–carbon bond formation by a Michael-type addition†‡

Katarzyna Świderek,[a] Anna Pabis[b] and Vicent Moliner*[c]

Received 2nd March 2012, Accepted 31st May 2012
DOI: 10.1039/c2ob25465d

A theoretical study of the Michael-type addition of 1,3-dicarbonyl compounds to α,β-unsaturated carbonyl compounds has been performed in the gas phase by means of the AM1 semiempirical method and by density functional theory (DFT) calculations within the B3LYP and M06-2X hybrid functionals. A molecular model has been selected to mimic the role of a base, which is traditionally used as a catalyst in Michael reactions, an acetate moiety to modulate its basicity, and point charges to imitate the stabilization of the negative charge developed in the substrate during the reaction when taking place in enzymatic environments. Results of the study of six different reactions obtained at the three different levels of calculations show that the reaction takes place in three steps: in the first step the α proton of the acetylacetone is abstracted by the base, then the nucleophilic attack on the β-carbon of the α,β-unsaturated carbonyl compound takes place generating the negatively charged enolate intermediate, and finally the product is formed through a proton transfer back from the protonated base. According to the energy profiles, the rate limiting step corresponds to the abstraction of the proton or the carbon–carbon bond formation step, depending on substituents of the substrates and method of calculation. The effect of the substituents on the acidity of the α proton of the acetylacetone and the steric hindrance can be analyzed by comparing these two separated steps. Moreover, the result of adding a positive charge close to the center that develops a negative charge during the reaction confirms the catalytic role of the oxyanion hole proposed in enzyme catalysed Michael-type additions. Stabilization of the intermediate implies, in agreement with the Hammond postulate, a reduction of the barrier of the carbon–carbon bond formation step. Our results can be used to predict the features that a new designed biocatalyst must present to efficiently accelerate this fundamental reaction in organic synthesis.

Introduction

Carbon–carbon bond formation, a challenging target in organic synthesis, is conventionally performed by nucleophilic displacements, radical additions or organometallic couplings.[1] In particular, a useful and efficient reaction is the Michael addition,[2] the conjugated addition of a resonance stabilized carbanion or another carbon nucleophile (Michael donor) to an activated α,β-unsaturated carbonyl-containing compound (Michael acceptor), as in Scheme 1. One of the most well-known carbon-Michael transformations is the base-catalyzed addition of ethyl acetoacetate to methyl acrylate.[3] It has been proposed that the acetoacetate is first deprotonated by the base, providing an enolate anion (Michael donor). Then, the enolate anion reacts in a 1,4-conjugate addition to the olefin of the acrylate (Michael acceptor). The carbonyl of the acrylate stabilizes the resulting anion until proton transfer occurs, regenerating the base. Overall, the rate determining step is proposed to be the attack of the enolate anion on the activated olefin.[4]

As mentioned, strong bases are traditionally used as catalysts for this reaction but undesired side-reactions such as eliminations,[5] polymerization of the Michael acceptor[6] or cyclocondensations[7] can take place. In order to avoid this problem, catalysts such as transition metals, lanthanide based compounds

Scheme 1 Schematic diagram of the Michael addition reaction.

[a]*Departament de Química Física, Universitat de València, 46100 Burjassot, Spain*
[b]*Institute of Applied Radiation Chemistry, Technical University of Lodz, 90-924 Lodz, Poland*
[c]*Departament de Química Física i Analítica, Universitat Jaume I, 12071 Castellón, Spain. E-mail: moliner@uji.es; Fax: (+34) 964-728066; Tel: (+34) 964-728084*

† This work is dedicated to the memory of our colleague and friend Prof. Purificación Escribano.

‡ Electronic supplementary information (ESI) available. See DOI: 10.1039/c2ob25465d

or the most recent application of modified enzymes by protein engineering can be employed.[8]

In the past decades, and mainly after the introduction of recombinant DNA technology, the use of enzymes for chemical transformations, including carbon–carbon bond formation reactions, is becoming a promising tool in organic synthesis laboratories of academia and industry.[9] Advantages of biocatalysts are due to their high efficiency, selectivity, fewer unwanted side-products, and their capability of working at mild conditions of temperature or pressure. These features justify the increasing interest in understanding and applying biocatalysts in producing high value chemicals from the environmental point of view. But also, the use of these new synthetic strategies opens the door to reducing the required reaction steps by using a one-pot procedure, allowing the decrease of energy consuming steps such as separation and purification of intermediates, with the obvious consequent economical savings. Challenges for one-pot transformations are centered on the design of highly selective catalysts with well-optimized isolated active sites. Heterogeneous catalysts are promising candidates to perform multistep processes,[10] particularly when different and incompatible active sites are required. In this case, the natural biochemical processes in living organisms are a major source of inspiration for design of new organocatalysts with high catalytic efficiency and stereoselectivity.

If either an inorganic compound or a protein is used as a scaffold to properly shape an efficient catalyst, a deep knowledge of the reaction mechanism at a molecular level is required. In this regard, computational chemistry techniques have demonstrated to be an adequate complementary tool to explain, predict and guide organic synthesis experiments based on theoretically predicted reaction mechanisms. In the present study, the Michael-type addition of two different 1,3-dicarbonyl compounds to three different α,β-unsaturated carbonyl compounds, as depicted in Scheme 2, has been studied in the gas phase. These reactions are the ones studied experimentally by Berglund and co-workers in the presence and absence of enzymes (the wild-type and a modified *C. antarctica* lipase B).[11] Keeping in mind the molecular model we are using in this study, the experimental data will be considered as an upper limit of our predicted rate constants derived from the rate limiting step of the proposed molecular mechanism. The analysis of the geometrical and electronic features of the species appearing along the reaction paths of the different studied reactions will be used to explain the Michael addition reaction and to rationalize the design of an optimum catalyst.

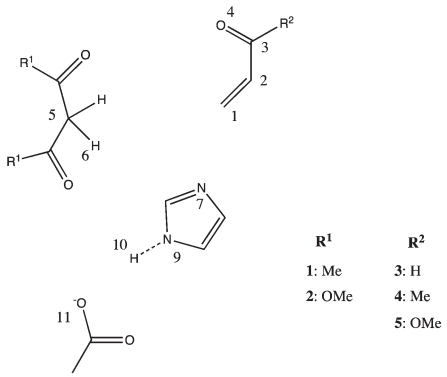

Scheme 2 Molecular model employed to study the Michael-type additions of 1,3-dicarbonyl compounds to α,β-unsaturated carbonyl compounds.

Computational methods

The theoretical study of six different Michael-type addition reactions has been performed within six different molecular models by changing the R1 and R2 substituents, as presented in Scheme 2. Imidazole has been used as a base, together with an acetate ion to modulate its proton affinity. This reduced model, depicted in Scheme 2, has been selected to mimic the conserved aspartate and histidine residues found in the active site of α/β hydrolases, which have shown significant activity for Michael addition reactions. The potential energy surfaces (PESs) for the 6 different reactions have been obtained at the AM1 semiempirical level[12] and by means of density functional theory (DFT) with hybrid functionals such as B3LYP[13] and M06-2X.[14] The highly parametrized M06-2X hybrid functional was selected in order to improve the limitation of the dispersion treatment of the B3LYP functional. The 6-31+G** basis set was used for the DFT calculations.

After localizing the stationary points, frequency calculations were carried out to verify that the structures represent true minima or first-order saddle points on the gas phase PESs. Once first-order saddle points were located and characterized, the Intrinsic Reaction Coordinate (IRC) path was traced down from the saddle points to the corresponding minima using the full gradient vector. The global r.m.s. residual gradient in the optimized structures was always less than 0.04 kcal mol^{-1} $Å^{-1}$. It is important to note that no constraints were applied to any of the geometry optimizations. Although allowing more reliable energetics, this implies that possible artifacts, such as odd interaction complexes, can be obtained. Thus, proper orientation of the different structures in the starting point structures is a crucial step in the computational protocol. Also, keeping in mind that the reaction under study is a multi-step process, IRC calculations traced forward from a TS structure do not necessarily converge in the end of the backwards path traced from the following IRC. In this sense, efforts have been made to get a converged result, otherwise the minimum energy structure, belonging to the reaction path, was selected. Zero point energies and thermal contributions to the enthalpy and to the free energy were obtained at 298 K by means of the M06-2X functional within the rigid-rotor and harmonic approximation in the gas phase.[15] Natural population analysis has been performed for all stationary structures.[16] All calculations were performed with Gaussian 09.[17]

Results and discussion

A schematic representation of the stationary point structures located along the reaction path traced on the PESs is depicted in Fig. 1, the potential energy profiles for the 6 studied reactions are presented in Fig. 2 while the comparison between the potential energy profiles and the free energy profiles obtained at the M06-2X level is shown in Fig. 3. It is important to point out that

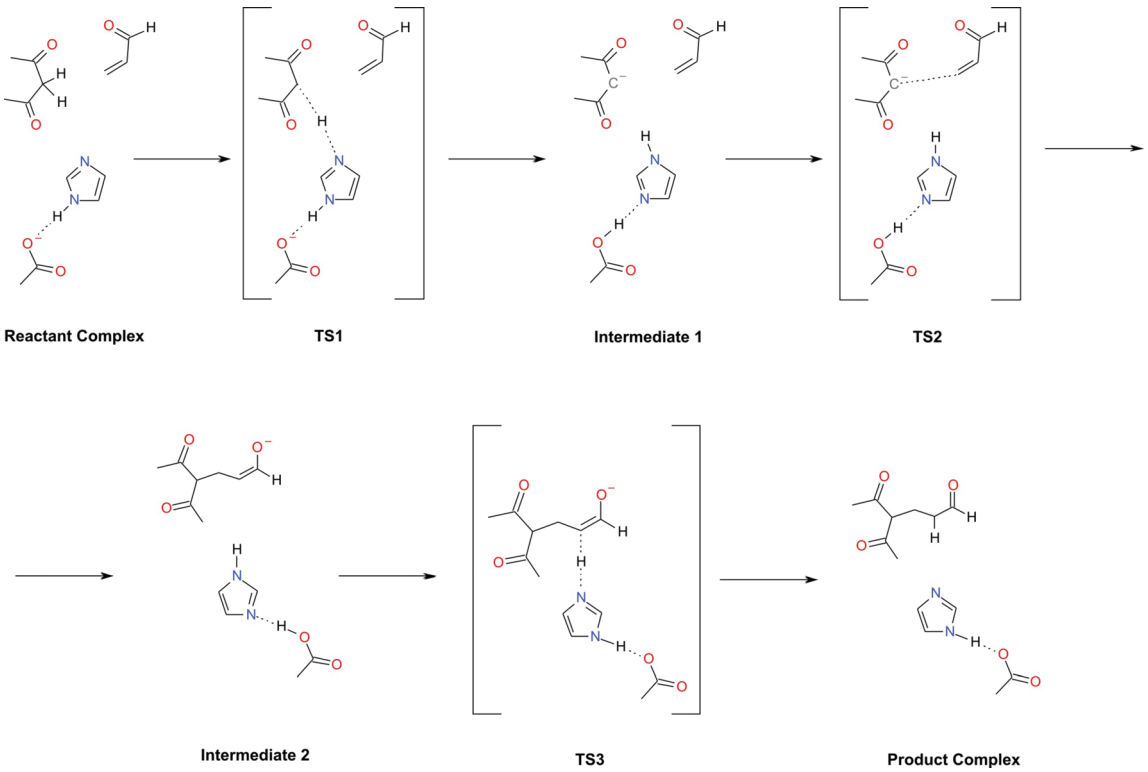

Fig. 1 Schematic representation of the stationary point structures located along the reaction path traced on the PESs.

free energies computed from normal mode analysis of cluster model systems in the gas phase are obviously related to just the explicit molecular system and, consequently, differences can appear in future studies in condensed media. Selected key inter-atomic distances for the stationary point structures located on the different PESs at the three levels of theory and relative energies to the reactant complex are reported in the ESI.‡

The first conclusion that can be derived from the reaction profiles is that the three theoretical methods describe all reactions as three step mechanisms. The fact that the reaction mechanism was qualitatively equivalent at high level and low level of theory (DFT and semiempirical methods, respectively) can be used in future studies of this reaction in the presence of a catalyst such as an enzyme. These studies required the use of expensive hybrid quantum mechanical/molecular mechanics (QM/MM) molecular dynamics (MD) simulations, in which, due to computational limitations, QM regions are necessarily described by low level semiempirical Hamiltonians. Nevertheless, it is also important to note that, as is discussed in detail below, the relative energy barriers, and consequently the rate limiting step (RLS) of the full process, depend on the level of calculation and in the inclusion of entropic contributions.

Interestingly, when exploring the transformation from reactant complex to the second intermediate by means of a two dimensional PES, explicitly controlling the C1–C5 distance and the proton transfer from C5 to N7, a not very much higher in energy concerted path could be traced, as shown in Fig. 4 for reaction 1 + 3 (see ESI‡ for the corresponding PESs for the rest of the reactions showing the same feature). This result can suggest that a protein environment could slightly change the topology of the potential or free energy surfaces, making feasible a reaction mechanism involving fewer chemical steps. Nevertheless, no stationary point corresponding to a saddle point of order one can be located on the gas phase surface for this possible concerted path. Thus, the reaction mechanism in the gas phase is described as follows: in the first step the α proton of the acetylacetone is abstracted by the base, then the nucleophilic attack on the β-carbon of the α,β-unsaturated carbonyl compound takes place generating the negatively charged enolate intermediate, and finally the product is formed through a proton transfer back from the protonated base.

The catalytic dyad formed by the imidazole and acetate provides a unique function in shuttling protons back and forth in the sequence of reaction steps. This feature of the catalytic acid–base dyad to serve either as a Brønsted acid or as a Brønsted base, when found in the conjugate base form, has been recently used by Yang and Wong to design a new type of chiral β-amino acid organocatalyst.[18] This was based on a carboxyl and imidazole pair that catalyzes Michael additions of aldehydes to nitroalkenes. In fact, as mentioned in the introduction section, we introduced the two moieties in the model to mimic the conserved histidine–aspartate pair observed in the active site of enzymes catalyzing the Michael addition, such as *Candida antarctica* Lipase B (CALB).[11] Nevertheless, the system behaves in a different way if comparing the results obtained with different methods. Thus, AM1 calculations show a relative movement between the proton and the N9 and O11 atoms depending on the charge of the imidazole, but proton shuttling is not observed along the reaction process (see key inter-atomic distances obtained for all localized stationary point structures in the ESI‡).

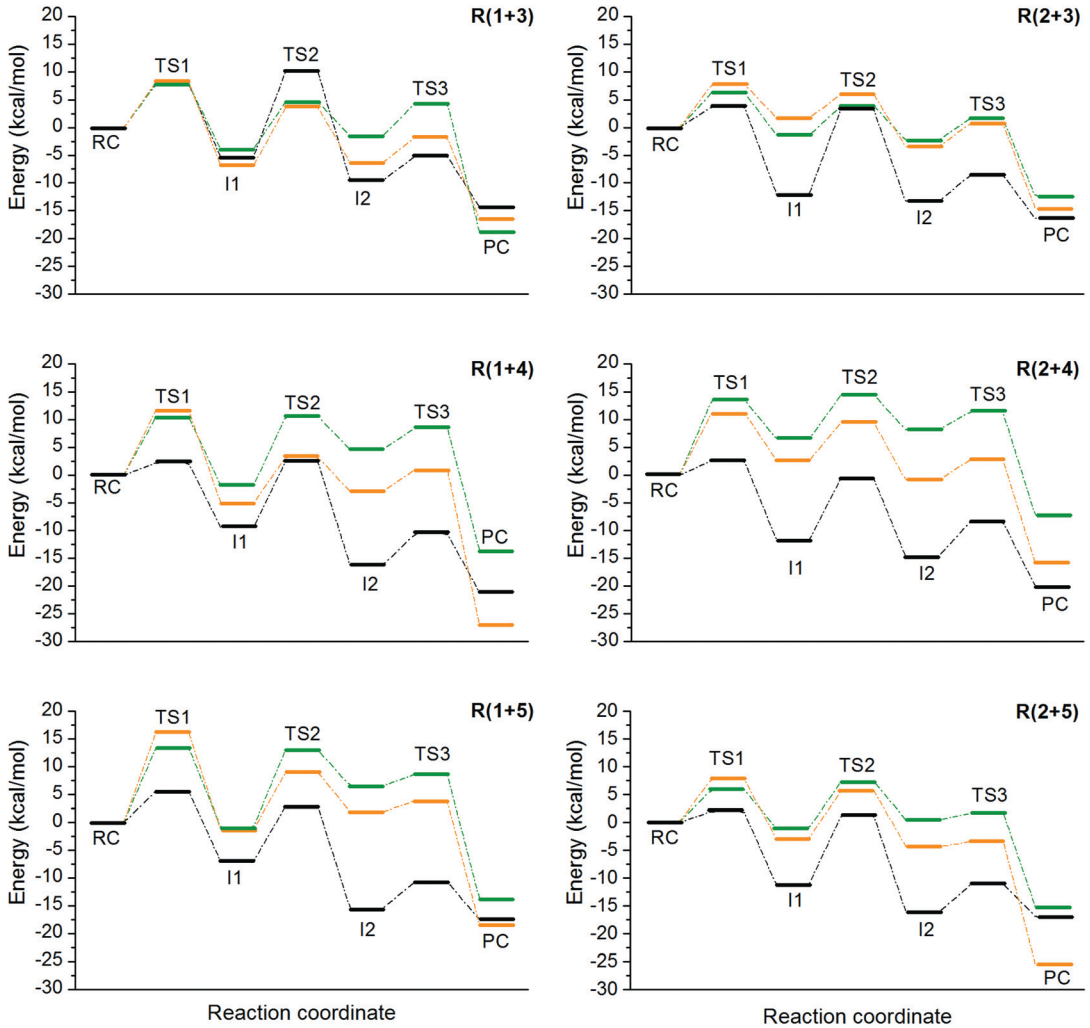

Fig. 2 Potential energy profiles for the Michael-type additions of 1,3-dicarbonyl compounds to α,β-unsaturated carbonyl compounds, as defined in Scheme 2, obtained at AM1 (black line), B3LYP (green line) and M06-2X (orange line) levels of calculation.

The proton is spontaneously transferred to the acetate in initial RC optimization and although H10–O11 suffers an elongation in RC and PC, concomitantly with an approach between donor and acceptor atoms, H10 proton is linked to the acetate all along the reaction profile. According to B3LYP calculations, H10 proton is initially bonded to imidazole in RC but it is spontaneously transferred to the acetate in the first step, remaining bonded to O11 until the last TS, when it goes back to the base concomitantly with H6 proton transfer from imidazole to the substrate. This behavior is observed in all reactions except in reaction 1 + 3, where H10 is initially bonded to acetate and remains in this position until the last step, as occurs in AM1 calculations. This behavior is equivalent to the one deduced from M06-2X calculations for reactions 1 + 3, 2 + 3, 2 + 4 and 2 + 5 while the shuttling of H10 proton is observed for reactions 1 + 4 and 1 + 5. These results reflect the labile character of this proton and the role of the imidazole–acetate pair that adapts to reach the minimum energy conformation, depending on the level of theory and the substituent of both 1,3-dicarbonyl compounds and the α,β-unsaturated carbonyl compounds favoring the abstraction of the α proton of the former. In fact, the energy barrier of this proton transfer, computed at the M06-2X level for a frozen geometry, reveals values lower than 2 kcal mol^{-1} in all systems. Our results show that the imidazole ring in AM1 structures of RC presents a negative charge that can be related with the systematically lower barrier of the first step by comparison with DFT results. DFT results do not allow such a direct conclusion. Thus, reactions with compound **1** follow the same trend, lower barriers are obtained when the proton is already attached to the acetate in RC (first barrier of reaction 1 + 3 is *ca.* 10 kcal mol^{-1}, while a value *ca.* 15 kcal mol^{-1} is obtained for reactions 1 + 4 and 1 + 5), but the same trend is not observed when analyzing reactions with compound **2**. Proton shuttling is observed from RC to TS1 in the three reactions of compound **2** studied by B3LYP, while H10 is already transferred to acetate in RC structures optimized with the M06-2X functional, also for the three reactions.

The second step, the carbon–carbon bond formation, presents energy barriers that are, in general, close to the ones observed for the first step. This step can be strongly favored if the negative charge developed on the oxygen atom of the α/β-unsaturated compound from I1 to I2 was stabilized by positive charges. This effect has been previously described as an oxyanion hole

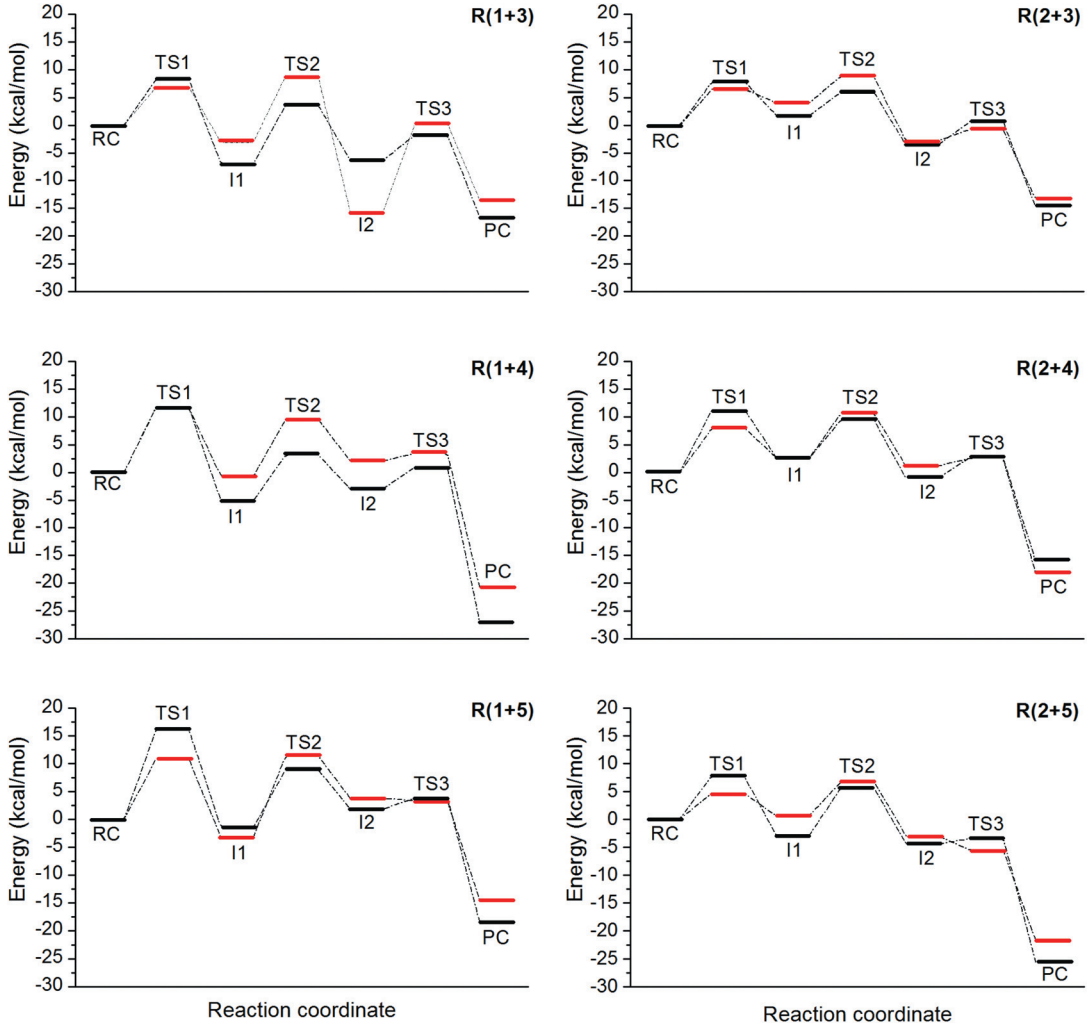

Fig. 3 Energy profiles for the Michael-type additions of 1,3-dicarbonyl compounds to α,β-unsaturated carbonyl compounds, as defined in Scheme 2, obtained as potential energy (black line) and free energies (red line) within the M06-2X functional.

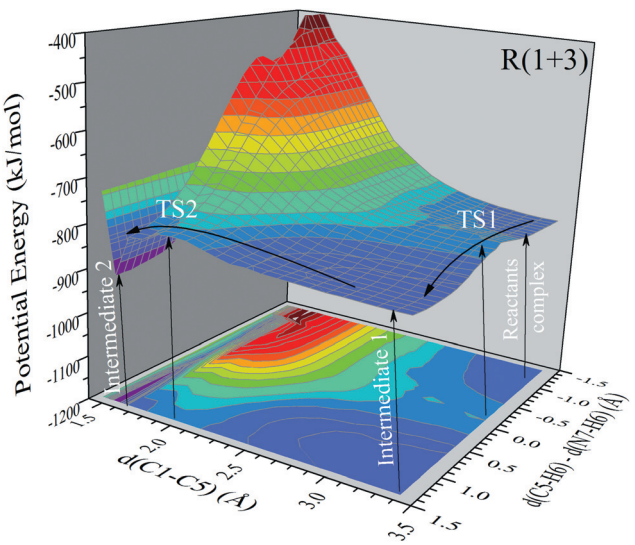

Fig. 4 Potential energy surface for the conversion from reactants to intermediate 2 for the 1 + 3 reaction obtained with the AM1 method.

stabilization in the case of enzyme catalyzed reactions such as serine proteases,[19–21] human acetylcholinesterase,[22] ketosteroid isomerase,[23] *etc*.

In order to check this hypothesis, single point energy calculations at the M06-2X level have been carried out with a positive charge located at 2.0 Å from the O4 atom, with the stationary point structures located on the PESs. The calculations for reactions 1 + 3 and 2 + 3, presented in Fig. 5, show a dramatic stabilization of I2 (in a range between 25 and 30 kcal mol^{-1}). In agreement with the Hammond postulate, this stabilization provokes a reduction of the energy barrier for the first step. In fact, according to the results, the I1 to I2 transformation becomes, under the effect of this positive charge, a barrier-less step. Obviously, such an effect would not be so dramatic in an enzyme active site where hydrogen bond interactions are established, with residues such as glycine and threonine, rather than interaction with positive point charges.

Regarding the third step, consisting of the proton transfer from the protonated imidazole to the unsaturated β-carbon of the substrate, its energy barrier can be modulated by the imidazole–acetate dyad, as was the case for the first step. Thus, for instance,

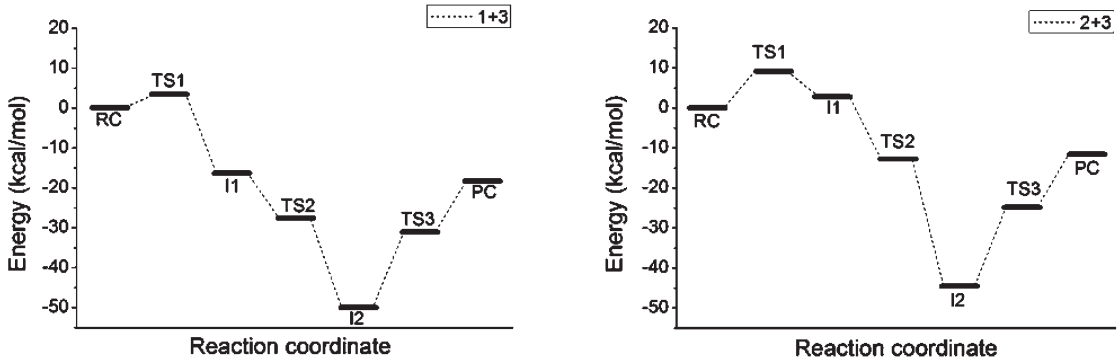

Fig. 5 Potential energy profiles for the Michael-type additions of **1** + **3** and **2** + **3**, as defined in Scheme 2, obtained at the M06-2X level with a positive charge at 2.0 Å from the O4 atom. See text for details.

the highest barrier for this step with DFT methods was obtained for reaction 1 + 3, while the lowest barrier was obtained for reaction 2 + 5. In the former, the variation of the N9–H10 distance from I2 to TS3 is 0.088 and 0.070 Å at the B3LYP and M06-2X levels, respectively, while the corresponding distance for reaction 2 + 5 changes just by 0.071 and 0.045 Å, respectively (see ESI‡ for the list of key inter-atomic distances obtained at all levels of theory). These results suggest a correlation between the activity of this dyad and the energy barrier, an effect already observed in the first step. In fact, the computed proton affinities for the imidazole appear to be significantly lower than those corresponding to the imidazole–acetate dyad (see ESI‡). This result would suggest that the acetate moiety could help in reducing the barrier of the first step. According to these findings, we could expect that the structure and motions of an enzyme capable of catalyzing this kind of reaction must be in such a way that the relative positions of histidine and aspartate (the two conserved residues localized in the active site of CALB, for instance) favor the proton transfer to, and from, the base (histidine), by reducing the energy barrier. Another important effect in this last step is, as discussed previously, the possible stabilization of the I2 by an oxyanion hole in the enzyme active site by partially neutralizing the charge developed on the O4 oxygen atom in the second step. This effect would slightly increase the barrier of the last step, since negative charge on this atom is neutralized from I2 to products. This non-favorable effect, if dramatic, could provoke the last step to become rate limiting. Nevertheless, these results must be analyzed from a qualitative point of view, keeping in mind the kind of calculations performed to obtain the perturbed profiles. Moreover, tautomers, such as the enol tautomers of the 1,3-dicarbonyl compounds, can appear under the effect of a protein environment and this would open the possibility of competing reactions. This structure can appear also in the gas phase in reactants if the initial structures are not properly prepared, and also in the products state if the reaction coordinate used to explore the reaction is not adequately selected. Transformation from 1,3-dicarbonyl to the enol tautomer requires breaking and forming bonds (transfer of a hydrogen from the α-carbon to the carbonyl oxygen) that, at least in gas phase calculations, imply a non-negligible energy barrier and thus this effect can be avoided.

Overall, the three step mechanism obtained for all 6 reactions is different to the two step mechanisms proposed for similar reactions catalyzed by enzymes, such as the ping-pong mechanism of the hydrolysis of methyl acrylate to acrylic acid catalyzed by wild-type *Pseudozyma antarctica* lipase B (PalB),[24] the Michael addition of acetylacetone to methyl acrylate catalyzed by Ser105Ala PalB mutant,[24] or the direct epoxidation of the unsaturated aldehyde mechanism in *Candida antarctica* Lipase B (CALB).[25] Also, this mechanism is different from the aldol addition of acetaldehyde or acetone studied by quantum mechanical calculations in the gas phase with a cluster model mimicking the CALB activity.[8] In all these cases, the proton abstraction and the C–O or C–C bond formation, depending on the reaction, would take place concertedly. According to our theoretical predictions and as discussed before, the enolate ion, I1, is a local minimum in all studied reactions obtained with the AM1 semiempirical Hamiltonian and with the two functionals B3LYP and M06-2X. This result, in contrast to previous studies that render two step mechanisms, opens the possibility of distinguishing two possible contributions to the total energy barrier that have been claimed to explain the trend of the experimentally measured rate constants:[11] the acidity of the α-protons of the acetylacetone derivatives and the steric hindrance of the β-carbon of the acrolein derivatives. Thus, according to our reaction profile, the importance of the former effect would be reflected in abstraction of a proton by the base, the height of the first barrier (TS1), while the latter would be measured by the barrier of the nucleophilic carbon addition step (TS2).

In order to further analyze the result from a kinetic point of view, and to determine the RLS, we must remember that for multi-step reactions, as stated by Murdoch,[26] the "fluid-flow analogy" (where the RLS acts as a "bottleneck" so that it is identified by the step with the highest energy forward barrier) is only valid for irreversible processes while associating the step presenting the highest energy TS as the RLS may fail for irreversible reactions where intermediates more stable than the reactants occur. Accordingly, it is interesting to observe that the highest energy forward barriers obtained with the semiempirical method correspond to the nucleophilic carbon addition step, characterized by TS2, in all cases (see Fig. 2 and Table S2 of the ESI‡). Reactions 1 + 3 and 1 + 4 present, in addition, the highest energy TS. The study of the reactions with the M06-2X functional shows that the highest energy TS corresponds to the proton abstraction for all reactions. Nevertheless, due to the stabilization of the first intermediate, the barrier of the second step is higher than that of the first step in reactions 1 + 3 and

2 + 5. Finally, in the case of the B3LYP functional, the first step presents the highest energy TS for reactions 1 + 3, 1 + 5 and 2 + 3, TS2 is the highest energy TS in reactions 2 + 4 and 2 + 5, and TS1 and TS2 appear to be degenerate in reaction 1 + 4. Regarding the energy barriers, due to stabilization of I1, the second step becomes the RLS in all reactions but 2 + 3.

All in all, according to the potential energy profiles, the RLS would correspond to the second step for all reactions under study with AM1 while DFT results provide different pictures: B3LYP dictates that the second step would be the RLS for all reactions but 2 + 3 where the first step would be the RLS, while according to M06-2X calculations, the first step is the RLS in all reactions but 1 + 3 and 2 + 5 where the rate of the process would be controlled by the second step. This conclusion is slightly modified when plotting the reaction profiles in terms of free energies, as shown in Fig. 3. The RLS is changed from step 1 to step 2 in reactions 1 + 5, 2 + 3 and 2 + 4 after including the ZPE and thermal corrections in the M06-2X profiles, and from step 2 to step 3 in reaction 1 + 3. If comparing the reactions with acetylacetone, **1**, with those reacting with dimethyl malonate, **2**, it could be concluded that the barriers of the first step of the reactions with the latter are lower than the reactions with acetylacetone, in terms of both potential and free energies. The methoxy substituent effects, which have been postulated to provoke a decrease of the acidity of the α-protons and then present a higher barrier for the proton transfer, are confirmed by the computed proton affinities of both molecules (see ESI‡). Nevertheless, this can not be used as a guide for the full reaction, according to our free energy profiles obtained with the M06-2X functional. The RLS of reactions with dimethyl malonate, **2**, is the second step for the three reactions while for reaction with acetylacetone, **1**, the RLS can be the first step (reaction 1 + 4) or third step (reaction 1 + 3), although as commented above, this last result can be due to an over-stabilization of the second intermediate.

Finally, it must be mentioned that any attempt to compare our theoretical results with the experimental non-catalyzed rate constant of the same reactions studied by Berglund and co-workers[11] must be done with caution since, as long as we are introducing an activated base molecule in our molecular model, the reactions cannot be considered completely as non-catalyzed. The free energy barriers that could be deduced from the rate constants obtained by Berglund and co-workers,[11] have to be considered as an upper limit for our model. In fact, the experimental free energy barriers, calculated in the context of the transition state theory, range from 23 kcal mol^{-1} (reaction 1 + 3) to more than 31 kcal mol^{-1} (reaction 2 + 5). We can also consider that, in order to compare our results with experimental data in solution, it would be necessary to estimate the free energy cost for association of the involved species to form the reactant complex at the same concentrations as those experimentally used. According to the volume analysis of Warshel and co-workers, the free energy cost of bringing two specific molecules next to each other in solution (that is 55 M in water) is *RT* ln 55, which renders a value of *ca.* 2.4 kcal mol^{-1} at room temperature.[27] The assumption that bringing the reactants together to form the reactant complex is an entirely entropic term, appears to be an accepted approximation but can lead to an underestimation of the free energy cost of prealigning the groups for catalysis in solution.[28] Thus our barriers computed from the reactant complex in vacuum have to be considered as a lower limit if comparisons have to be done with the reactions in solution. Adding the energy cost of association would bring our results closer to the experimental data.

Comparisons with the enzyme catalyzed reactions can not be straightforward neither as long as the enzyme active site can provoke specific interactions and constraints into the substrates that are not simulated with our method and model. Thus, for instance, an argument based on steric hindrance to explain a lower enzyme reactivity for dimethyl malonate **2** than acetylacetone **1** when reacting with acrolein **3** would not be supported by our calculations, but it does not necessarily mean that it was wrong.

Conclusions

A theoretical study of the Michael-type addition of 1,3-dicarbonyl compounds to α,β-unsaturated carbonyl compounds has been performed in the gas phase by means of the semiempirical AM1 Hamiltonian and the B3LYP and M06-2X hybrid functionals. A molecular model has been selected to mimic the role of a base which is traditionally used as a catalyst in Michael reactions, an acetate moiety to modulate the proton affinities of the base, and a positive point charge to stabilize the negative charge developed in the substrate during the process in enzyme catalyzed reactions. The exploration of the molecular mechanism in the gas phase can render information on the features that have to be present in a potential biocatalyst and consequently, the future rational design of new biocatalysts can benefit from the conclusions extracted from this systematic study. The results of six different reactions obtained at the three different levels of calculations show that the reaction takes place in three steps, in contrast to previous studies on similar reactions that suggest a two step mechanism. Nevertheless, PESs show the possibility of a not much higher energy path that could avoid some of the intermediates, a result that can be important in a protein environment. Nonetheless, according to our results obtained in the gas phase, in the first step the α proton of the acetylacetone is abstracted by the base, then the nucleophilic attack on the β-carbon of the α,β-unsaturated carbonyl compound takes place generating the negatively charged enolate intermediate, and finally the product is formed through a proton transfer back from the protonated base. The relative energies of the located stationary points depend on the method of calculation and, consequently, these have to be considered to arrive at general conclusions. According to the energy profiles, the rate limiting step corresponds to the abstraction of the proton or the carbon–carbon bond formation step, case depending. The free energy profiles obtained at the M06-2X level of calculation indicate that the rate limiting step for reactions with dimethyl malonate, **2**, would be the latter, while in one of the reactions with acetylacetone, 1 + 4, the abstraction of the proton would determine the rate of the process.

The effect of the substituents on the acidity of the α proton of the acetylacetone and the steric hindrance can be analyzed by comparing these two separated steps. The results show that the latter effect is not decisive in the final barriers of the rate limiting steps. A positive point charge located at 2 Å from O4 confirms the catalytic role of the oxyanion hole proposed in the enzyme

catalysing Michael additions. Stabilization of the intermediate would imply a reduction of the barrier of the second step.

Comparison of our predicted rate constants with experimental energy barriers deduced from rate constants measured for the corresponding catalysed and non-catalysed reactions has to be done with caution. Our reactions can not be considered as equivalent to a non-catalyzed reaction, since we are including some species that mimic the catalyst, neither to the enzyme catalysed reaction, since our model lacks the constraints imposed by the protein in the active site and the specific electrostatic interactions.

In conclusion, with these results in hand, an efficient biocatalyst should possess a strong base capable of abstracting the α-protons of the diketone, and favourable interactions with the O4 atom of the α,β-unsaturated carbonyl compound that develops a negative charge during the reaction.

Acknowledgements

We thank the Spanish *Ministerio de Ciencia e Inovación* for project CTQ2009-14541-C2, Universitat Jaume I – BANCAIXA Foundation for project P1·1B2011-23, Generalitat Valenciana for *Prometeo*/2009/053 project. The authors also acknowledge the Servei d'Informatica, Universitat Jaume I, Academic Computer Centre CYFRONET, AGH, Krakow, grant MNiSW/SGI3700/PLodzka/088/2009, for generous allotment of computer time. V. Moliner would like to thank the Spanish Ministry *Ministerio de Educación* for traveling financial support, project PR2009-0539.

References

1 E. Busto, V. Gotor-Fernández and V. Gotor, *Chem. Soc. Rev.*, 2010, **39**, 4504.
2 A. Michael, *Am. Chem. J.*, 1887, **9**, 115.
3 N. F. Albertson, *J. Am. Chem. Soc.*, 1948, **70**, 669.
4 B. D. Mather, K. Viswanathan, K. M. Miller and T. E. Long, *Prog. Polym. Sci.*, 2006, **31**, 487.
5 F. Fringuelli, G. Pani, O. Piermati and F. Pizzo, *Tetrahedron*, 1994, **50**, 11499; S. Saito and H. Yamamoto, *Chem.–Eur. J.*, 1999, **5**, 1959.
6 B. Alcaide and P. Almendros, *Angew. Chem., Int. Ed.*, 2008, **47**, 4632.
7 H. O. House, D. S. Crumrine, A. Y. Teranishi and H. D. Olmstead, *J. Am. Chem. Soc.*, 1973, **95**, 3310.
8 C. Branneby, P. Carlqvist, A. Magnusson, K. Hult, T. Brinck and P. Berglund, *J. Am. Chem. Soc.*, 2003, **125**, 874.
9 G. A. Strohmeier, H. Pichler, O. May and M. Gruber-Khadjawi, *Chem. Rev.*, 2011, **111**, 4141.
10 M. J. Climent, A. Corma and S. Iborra, *Chem. Rev.*, 2011, **111**, 1072.
11 M. Svedendahl, K. Hult and P. Berglund, *J. Am. Chem. Soc.*, 2005, **127**, 17988.
12 M. J. S. Dewar, E. G. Zoebisch, E. F. Healy and J. J. P. Stewart, *J. Am. Chem. Soc.*, 1985, **107**, 3902.
13 A. D. Becke, *J. Chem. Phys.*, 1993, **98**, 5648.
14 (*a*) Y. Zhao and D. G. Truhlar, *Theor. Chem. Acc.*, 2008, **120**, 215; (*b*) Y. Zhao and D. G. Truhlar, *Acc. Chem. Res.*, 2008, **41**, 157.
15 D. A. McQuarrie, *Statistical Mechanics*, Harper & Row, New York, 1976.
16 A. E. Reed, L. A. Curtiss and F. Weinhold, *Chem. Rev.*, 1988, **88**, 899.
17 M. J. Frisch, G. W. Trucks, H. B. Schlegel, G. E. Scuseria, M. A. Robb, J. R. Cheeseman, G. Scalmani, V. Barone, B. Mennucci, G. A. Petersson, H. Nakatsuji, M. Caricato, X. Li, H. P. Hratchian, A. F. Izmaylov, J. Bloino, G. Zheng, J. L. Sonnenberg, M. Hada, M. Ehara, K. Toyota, R. Fukuda, J. Hasegawa, M. Ishida, T. Nakajima, Y. Honda, O. Kitao, H. Nakai, T. Vreven, J. A. Montgomery Jr., J. E. Peralta, F. Ogliaro, M. Bearpark, J. J. Heyd, E. Brothers, K. N. Kudin, V. N. Staroverov, R. Kobayashi, J. Normand, K. Raghavachari, A. Rendell, J. C. Burant, S. S. Iyengar, J. Tomasi, M. Cossi, N. Rega, J. M. Millam, M. Klene, J. E. Knox, J. B. Cross, V. Bakken, C. Adamo, J. Jaramillo, R. Gomperts, R. E. Stratmann, O. Yazyev, A. J. Austin, R. Cammi, C. Pomelli, J. W. Ochterski, R. L. Martin, K. Morokuma, V. G. Zakrzewski, G. A. Voth, P. Salvador, J. J. Dannenberg, S. Dapprich, A. D. Daniels, Ö. Farkas, J. B. Foresman, J. V. Ortiz, J. Cioslowski and D. J. Fox, *GAUSSIAN 09 (Revision A.1)*, Gaussian, Inc., Wallingford CT, 2009.
18 H. Yang and M. W. Wong, *J. Org. Chem.*, 2011, **76**, 7399.
19 A. Warshel, G. Narayszabo, F. Sussman and J. K. Hwang, *Biochemistry*, 1989, **28**, 3629.
20 J. A. Gerlt and P. G. Gassman, *Biochemistry*, 1993, **32**, 11943.
21 Y. K. Zhang, J. Kua and J. A. McCammon, *J. Am. Chem. Soc.*, 2002, **124**, 10572.
22 A. Ordentlich, D. Barak, C. Kronman, N. Ariel, Y. Segall, B. Velan and A. Shafferman, *J. Biol. Chem.*, 1998, **273**, 19509.
23 A. Warshel, P. K. Sharma, Z. T. Chu and J. Aqvist, *Biochemistry*, 2007, **46**, 1466.
24 M. Svedendahl, B. Jovanovic, L. Fransson and P. Berglund, *ChemCatChem*, 2009, **1**, 252.
25 M. Svedendahl, P. Carlqvist, C. Branneby, O. Allnér, A. Frise, K. Hult, P. Berglund and T. Brinck, *ChemBioChem*, 2008, **9**, 2443.
26 J. R. Murdoch, *J. Chem. Educ.*, 1981, **58**, 32.
27 J. Villa, M. Strajbl, T. M. Glennon, Y. Y. Sham, Z. T. Chu and A. Warshel, *Proc. Natl. Acad. Sci. U. S. A.*, 2000, **97**, 11899.
28 P. A. Kollman, B. Bernd Kuhn and M. Pera1kyla, *J. Phys. Chem. B*, 2002, **106**, 1537.